AUTOMATED SPLAY ANGLE CALCULATION FOR LINE ARRAY LOUDSPEAKER SYSTEMS

Ambrose Thompson Martin Audio Ltd

1 INTRODUCTION

Vertically arrayed loudspeakers systems are currently the predominant technique used in large and medium scale touring sound systems. Due to the complex nature of elemental interactions a wealth of CAD tools are available that predict the output of a given array or combination [[4], [2], [3]]. To design an array with these tools the user manually alters the splay angles and inspects the output, this process is repeated until an acceptable output is achieved. Some of the factors important to the success of the manual method of array design are:

1. Accuracy of the radiation model.
2. The user's mental model of the system [8].
3. Speed of performance feedback.
4. Size and granularity of the domain.
5. Time available.

The aim of this article is to investigate a method which attempts to remove the user from having to manually iterate toward a desired sound-field. Whether manual or automatic design is employed some of the above factors are common and will be examined.

2 2D / 3D

Many users of CAD systems tasked with manual design of vertical arrays only evaluate the performance on a thin strip normal to the front of the array. This method allows relatively rapid feedback when compared to full audience plane calculation. Good performance on the strip generally reflects in good performance in the full calculation, assuming good broadband horizontal pattern control. We will follow this convention for now and later discuss how to incorporate points outside the strip, whilst still avoiding a full calculation.

3 SIMPLE RADIATION MODEL

The simple radiation model has been termed the directional point source model and forms the basis for practically all array CAD tools. Pressure at the receiver points $\mathbf{r}$ is formed from the complex summation of all elemental sources. Each elemental source has an associated measured complex 'balloon' of pressure at N_f frequencies $\mathbf{f}$ and an orientation. The computation defines a ray from each source to each receiver point, the pressure where the ray intersects the balloon is determined

via a complex interpolation of nearby points; this pressure $P(\mathbf{r},\mathbf{f})$ is then propagated to the receiver point [9].
This model assumes that the measured data for each source is obtained in the far-field for that source and that the presence of neighbouring enclosures is not significant, since neighboring enclosures are seldom present when source measurements are performed. Despite the latter assumption the simple model is thought to give a good indication of the expected pressure at the receiver points.

4 VALIDITY OF RADIATION MODEL

We can already guess where the simple radiation model is valid, i.e. when we are well into the light like region of geometric acoustics for a single element [5]. In addition at very low frequencies where omni directional radiation is nearly achieved. Therefore it is likely that the model is valid at the upper end of the pass band of each frequency section and at the very low frequencies of the lowest pass band. Outside of these intervals the neighbouring cabinets are likely to have a substantial influence, what we seek to find is the magnitude of this influence. If we compare the performance of one isolated element to that of each array element measured with its neighbours present we can indicate this influence.

Line arrays are difficult to measure as a system. The physical handling presents a sizable obstacle to achieving the highly accurate positioning required. Further difficulties regarding environmental and other measurement related issues are discussed in [11]. For these reasons a scaled down version of a line array system was constructed where each element is only $55mm$ high and houses a single $45mm$ full range (100-20000 Hz) drive unit. The array consisted of 8 such elements arranged in a progressively curved configuration as shown in Fig 1. The left column of Fig 2 shows the vertical hemispherical polar output of such a measurement conducted at 4 metres. Not shown is the on axis level which fluctuates with frequency being between 3-6 dB louder in the region where the polars are different to the isolated element.

Arrays can be modeled as an exterior problem of a boundary element method (BEM) [6]. It would be useful not to have to measure each configuration of splay angles and array length when determining the influence of neighbouring elements. The scaled array has been analysed using this method. The right column of Fig 2 shows results at equivalent positions to the measurements taken, note different frequency limits to the measured graphs.

From the measurements and the BEM analysis it may be possible to deduce the frequency above which the neighbouring elements have little influence. For the isolated element this frequency is such that the pressure amplitude has dropped, relative to the main axis, by at least 15dB at right angles to the main axis.

5 PARAMETERS AND VARIABLES

Consider a particular vertical array of N identical uniformly excited elemental loudspeakers characterised by a set of splay angles $\mathbf{x}$ at a fixed position in a venue. The venue is defined by a set of N_a audience receiver positions $\mathbf{r}_a$ and N_{na} non-audience receiver positions $\mathbf{r}_{na}$. We can view the resultant pressure as a function of the splay angles (a parameter) and the independent variables of frequency and receiver position $P(\mathbf{r},\mathbf{f},\mathbf{x})$.

The spatial variable is divided into intervals in the region of $0.1m$ to $1.0m$. This resolution captures the special detail adequately in practice. Frequency is divided into $\frac{1}{36}$th octave bands and is deemed fine enough for representing most frequency responses.

6 ABSTRACT VIEW OF RESULTS

The normal presentation of performance along the strip to the user either employs overlaid frequency responses at different receiver points, or overlaid plots of pressure at the receiver points for different frequencies (distance plots). Both of these views become cumbersome when more than 10 graphs are overlaid and unworkable when frequency and receiver points number 100 or more.

What is required is to be able to view the pressure at all receiver points and at all frequencies. This can be achieved with a 3D plot where the x axis represents frequency, the y axis receiver position index and the z axis pressure. Conceptually it is like stacking up all the frequency response plots along the y axis, or indeed all the distance plots along the x axis. A contour plot is then formed from the pressure amplitude values. Using this view the result of any change is seen across the entire range of frequency and position. We will term this type of plot 'Enhanced 2D' (E2D) and use it throughout this document. Note that index position 1 maps to the first receiver position of the nearest audience plane to the array and then increases in an anticlockwise sense, eventually arriving to a point above the array. Plane boundaries are marked with dashed white horizontal lines.

7 THE ARRAY

The array comprises of 20 identical elements each $115mm$ high containing an HF and LF section in close proximity, polar performance for a single element is shown in Fig 3. The maximum splay between elements is 6 deg and the minimum is 0 deg with 0.5 deg steps available in this range. Signal processing consists of 2 FIR filters, one per frequency section, that provide response equalisation and a 'brick wall' crossover between the sections as in Fig 4.

8 DIRECT SEARCH OPTIMISATION METHODS

Optimisation is a branch of mathematics which encompasses a vast range of techniques that attempt to find the N parameters $\mathbf{x} \in R^N$ that minimise an objective function $\varepsilon(\mathbf{x})$ optionally including constraints on the parameters. A simple classification between the techniques is whether the algorithm uses the gradient of the objective function in order to determine the direction of the search in the search space. One such class of algorithm which does not is the 'generalised pattern search' described in an introductory manner in [12] and analysed further in [1]. The method can be viewed as an adaptive grid search over the search space where the grid or mesh $\mathbf{M}$ is defined by the mesh size, $\Delta \in R_+$ and a set of directions $\mathbf{D} \subset R^N$ whose positive linear combinations span R^N. Candidates for function evaluation can be determined by the user or a more structured approach of polling neighbouring points. A typical sequence of steps taken by a pattern search algorithm is shown in Algorithm1.

Algorithm 1 pattern search

Require: x_k , Δ_k for $k = 1$

```
while Stopping criteria not met do
  SEARCH : Perform a global search from the search
  point anywhere on M_k either heuristically or with
  some knowledge of the model to decide candidates for
  evaluation
  if improved mesh point found (ε(x_{k+1}) < ε(x_k)) then
    Optionally increase the mesh size (Δ_{k+1} ≥ Δ_k)
    search point becomes this improved point
    break
  else
    POLL : look at neighbouring points in the mesh
    if improved mesh point found (ε(x_{k+1}) < ε(x_k)) then
      search point becomes this improved point
      break
    else
      Reduce mesh size (Δ_{k+1} < Δ_k)  {This point is a mesh
      local optimiser}
      search point becomes this point
      break
    end if
  end if
  increment k
end while
```

At what point should we stop iterating? Time, mesh size, relative change in objective function or an absolute value of the objective function can all be used for stopping criteria. Simply because the relative change in objective function value, for example, disappears beneath the precision of our computation, it does not guarantee that we have arrived at a global minimum. The concept of global optimality keeps many mathematicians awake at night, but is of less significance to engineers who are most interested in obtaining a significant improvement in performance in a timely manner.

9 OBJECTIVE FUNCTIONS

In order to perform any numerical improvement via splay angle manipulation a measure of performance needs to be established. This is the purpose of the objective function defined above and it is required to return just one real positive number. Thus we need a target against which the current performance is compared or need to evaluate some other property of the current performance. In terms of pressure amplitudes on audience plane sections we may desire the same fixed value everywhere at all frequencies, or perhaps choose to minimise the partial derivatives with respect to frequency or position on our result surface.

Our experience has demonstrated that uniform pressure amplitude at every position and frequency is not a very useful target for live events, since it conflicts with audiences' psycho acoustic expectations. The target pressure amplitude $P_{targ}(\mathbf{r}_a, hbff)$ used throughout this paper varies only on the N_a points of $\mathbf{r}_a$ and is constant with the N_f frequencies $\mathbf{f}$. A target shape is set by choosing a 'mix' position r_{mix} at some point away from the array on the audience plane section, then levels relative to this at the extremes of coverage on the audience plane section, ΔP_{start} and ΔP_{stop}. In between each extreme point and the mix position the target pressure has a constant gradient. Typical values create a target that progressively drops in amplitude with increasing distance from the array.

The combined objective function $\varepsilon(\mathbf{x})$ is given in Eq9, where c_n controls the relative importance of the various components of the objective function. Note the evaluation of $P(\mathbf{r}_a, \mathbf{f})$ produces a N_a by N_f sized matrix $[\mathbf{Pa}]$ since the arguments are vectors, similarly $P(\mathbf{r}_{na}, \mathbf{f})$ produces a N_{na} by N_f matrix $[\mathbf{Pna}]$.

The component, ε_{leak} is a measure of 'leakage' defined by the ratio of total pressure present on non-audience positions to that present on audience positions and given in Eq1.

$$\varepsilon_{leak} = \frac{\sum_{j=1}^{j=N_{na}} \sum_{k=1}^{k=N_f} [\mathbf{Pna}]_{j,k}}{\sum_{j=1}^{j=N_a} \sum_{k=1}^{k=N_f} [\mathbf{Pa}]_{j,k}} \tag{1}$$

The main target component ε_{targ} given in Eq3 allows the shape to 'float' slightly, since it is the shape that is important rather than some absolute level. Each time a new array configuration is calculated a value for the mean pressure amplitude with frequency is determined at r_{mix} Eq2, the target is then defined relative to this value. Evaluation of the target $P_{targ}(\mathbf{r}_a, \mathbf{f})$ produces a N_a by N_f matrix $[\mathbf{Ptarg}]$, j_{mix} is the position index of r_{mix}.

$$mean_{rmix} = \frac{\sum_{k=1}^{k=N_f} [\mathbf{Pa}]_{j_{mix},k}}{N_f} \tag{2}$$

$$\varepsilon_{targ} = \frac{\left\| mean_{rmix} + [\mathbf{Ptarg}] - [\mathbf{Pa}] \right\|_2}{\sqrt{N_a}} \tag{3}$$

We would also like a measure of the flatness of the frequency response at each point in $\mathbf{r}_a$. For each point the mean pressure amplitude over frequency is calculated Eq4 resulting in a vector. This is expanded to a matrix of the same size as $[\mathbf{Pa}]$ Eq6, which forms part of the component ε_{fresp} given in Eq5

$$mean_j = \frac{\sum_{k=1}^{k=N_f} [\mathbf{Pa}]_{j,k}}{N_f} \quad j = 1 \ldots N_a \tag{4}$$

$$\varepsilon_{fresp} = \frac{\left\| [\mathbf{Pf}] - [\mathbf{Pa}] \right\|_2}{\sqrt{N_a}} \tag{5}$$

where $[\mathbf{Pf}]$ is given by

$$[\mathbf{Pf}]_{j,k} = mean_j k = 1 \ldots N_f,\ j = 1 \ldots N_a \tag{6}$$

The components $\varepsilon_{\frac{\partial P}{\partial f}}$ and $\varepsilon_{\frac{\partial P}{\partial r}}$ are measures of the size of the numerical partial derivatives of $P(\mathbf{r}_a, \mathbf{f})$ given in Eq 7 and Eq8.

$$\varepsilon_{\frac{\partial P}{\partial f}} = \frac{\left\| \frac{\partial P(\mathbf{r}_a, \mathbf{f})}{\partial f} \right\|_2}{N_a} \tag{7}$$

and

$$\varepsilon_{\frac{\partial P}{\partial r}} = \frac{\left\| \frac{\partial P(\mathbf{r}_a, \mathbf{f})}{\partial r} \right\|_2}{N_a} \tag{8}$$

and not investigated in this paper, thus c_4 and c_5 are set to 0.

$$\varepsilon(x) = c_1 \cdot \varepsilon_{targ} + c_2 \cdot \varepsilon_{fresp} + c_3 \cdot \varepsilon_{leak} + c_4 \cdot \varepsilon_{\frac{\partial P}{\partial f}} + c_5 \cdot \varepsilon_{\frac{\partial P}{\partial r}} \tag{9}$$

10 IMPROVED ARRAYS

In this section we apply the generalised pattern search to the splay angles parameter for a uniformly driven full size array in the venue shown in Fig 5, values for ΔP_{start} and ΔP_{stop} are $+6$ dB and -6 dB respectively. Given the observation relating the lower frequency limit for which the radiation model is valid to the polar performance of an isolated element we limit the optimisation to above 2000Hz.

For comparison a set of splay angles was determined manually in an effort to achieve a particular target. The results for this manual array are shown in the left column of Fig 6 as an E2D plot and as a frequency response at several position indices. In this configuration and the numerically improved version to follow we use some general knowledge of the model. We know that the array is likely to be more curved further down and that we should aim the top box in the vicinity of the coverage stop position. A 'progressive' curvature of the array is enforced by splitting the array into 7 sections, one for each major division of the splay angle range. From top to bottom each section allows only one splay angle starting at 0 and ending at 6 in the last section. The array is defined by what proportion of the total number of elements is in each section; note there could be no elements in a section if desired.

Displayed in the right column of Fig 6 is the improved version where the only component of the objective function was ε_{targ} i.e. $c_2 \ldots c_5 = 0$. The pattern search algorithm took 70s to perform the 7 iterations in which 81 function evaluations were calculated. The routine was halted when a minimum mesh size had been reached, other runs allowing smaller meshes did not result in significantly better solutions. The starting point for the run was that of the manual array.
The effect of including ε_{leak} is shown in Fig 7 as E2D plots; displayed first is the manual array and then three plots with increasing values of c_2.

What if the convex constraint is removed? If we allow the pattern search to operate directly on the splay angles we may observe this. Starting from the manual array the left column of Fig 8 shows the

array produced for direct manipulation of the splay angles in the same format at Fig 6, again using only the ε_{targ} component of the objective function. The right column of Fig 8 shows the array produced for direct splay manipulation including the ε_{targ} and the ε_{fresp} components of the objective function. The routine used a mesh size and time limit stopping criteria. After 20 minutes and over 1300 function evaluations the routine was stopped. Other runs allowing more time produced little further improvement before being stopped by the mesh size criteria. Splay angles resulting from all the calculations made can be viewed in Table 1.

11 DISCUSSION

The convex constrained array optimistaion produced a solution very rapidly; the target was closely met with a good frequency response over the audience area. Direct splay manipulation produced a configuration which was numerically better at achieving the target than the convex array, though with a less consistent frequency response. Including a desire for a flatter frequency response into the direct splay manipulation traded meeting the target pressure against response smoothness. This final array has the most consistent frequency response at the expense of deviating a little from the target. It was shown that the target can also be traded against sound field leakage. Of course, there are many other combinations of the objective function weights and only a few have been presented.

The requirement to limit the improvement to above a certain frequency due to flaws in the radiation model needs to be addressed. There has been some activity toward increasing the accuracy of simple radiation models in the middle frequencies, [10] for example modifies the elemental polars or straight low frequency arrays by an average value. An analytic approach in [7] is demonstrated for simple geometry though not extended to complex geometry. A more general numerical and fast method is currently being developed.

The venue shape used throughout is quite a simple one and is known to be amenable to progressively curved line arrays. More complicated venues where a progressive curvature array is less suitable are likely to display the usefulness of direct splay angle manipulation. A convex constrained array optimization may provide a good starting point for the more time consuming direct splay manipulation in such a venue. The convex constrained optimization is relatively insensitive to the shape of the array at the start of the process, generally pointing the top box at coverage stop is a good enough starting point.

The problem presented in this paper was deliberately quite simple. The main purpose was to assess the usefulness of the objective function, however real array deployment involves more than just setting the splay angles quickly. The method could be extended to include some of these, namely:

- Multiple sections at different horizontal angles through the audience planed to take into account off axis performance.
- Weighting of particular frequency intervals or audience portions to focus improvement to these areas.
- More flexible pressure target shapes, perhaps an interpolated curve of user defined values.
- Application to other types of array, for example more traditional cluster techniques or more broadly spaced arrays where position and orientation are not intrinsically linked.
- Including more parameters, for example array height, number of elements, element type etc.
- Block and box level EQ settings.

12 CONCLUSION

With the aid of an optimizer and a multi term objective function a useful level of abstraction from some of the parameters that govern the radiation behaviour of loudspeaker arrays was achieved. Improved radiation models are required before optimization techniques are applied over the entire frequency range.

13 REFERENCES

[1] C. Audet and J. Dennis. Analysis of generalized pattern searches.TR00-07 Department of Computational & Applied Mathematics, Rice University, Houston TX., 2000.
[2] CATT, CATT-Acoustic. http://www.catt.se/.
[3] DISPLAY, Martin Audio. www.martin-audio.com.
[4] EASE, ADA. www.ada-library.de.
[5] K Uno Ingard and P.M. Morse. Theoretical Acoustics. Collins, 1970.
[6] S. Kirkup. The Boundary Element Method in Acoustics. ISS, 1998.
[7] C. Pignon, C. Combet, P. Bauman, M. Urban, C. Heil The distributed edge dipole (DED) model for cabinet edge diffraction effects. Journal of the Audio Engineering Society, 52, 2004
[8] D.A. Norman. The Design of Everyday Things. The MIT Press, 1998.
[9] H. Staffeldt. Prediction of sound pressure fields of loudspeaker arrays from loudspeaker polar data with limited angular and frequency resolution.108th Convention of the Audio Engineering Society, Preprint :5130, 2000.
[10] E. Start. Optimisation of DDS-controlled loudspeaker arrays using a hybrid PSM-BEM model. 21st Reproduced Sound Conference of the IOA, 2005
[11] H. Staffeldt A. Thompson. Line array performance at mid and high frequencies. 117th Convention of the Audio Engineering Society, Preprint:6274, 2004.
[12] J.E. Dennis J. Virginia. Derivative-free pattern search methods for multidisciplinary problems. American Institute of Aeronautics and Astronautics, pages 922–932, 1994.

14 FIGURES

1 Scaled array on top of a Martin Audio W8L Longbow.
2 Vertical hemispherical polars of measured [200-20000] Hz and BEM simulated [200-10000] Hz for scaled array elements with neighbours. Each colour change is 3dB.
3 Vertical and horizontal hemispherical polars for HF and LF section of full sized element.
4 Signal processing applied each element.
5 Diagram of receiver positions.
6 Manual array vs optimized. Optimised array has convex constraint. Each colour change is 3dB. Red line = Target SPL. Green line = Average SPL.
7 Effect of combining the target and leakage component.
8 Direct splay angle manipulation optimized arrays. Each colour change is 3dB. Red Line = Target SPL. Green Line = Average SPL.

15 ACKNOWLEDGEMENTS

The author would like to thank Richard Cheney of Martin Audio for the initial suggestion of applying optimization to line array splay angles and Glenn Leembruggen for helpful discussions regarding the importance of a consistent frequency response.

Figure 2 Vertical hemispherical polars of measured [200-20000]Hz and BEM simulated [200-10000] Hz for scaled array elements with neighbours. Each colour change is 3dB.

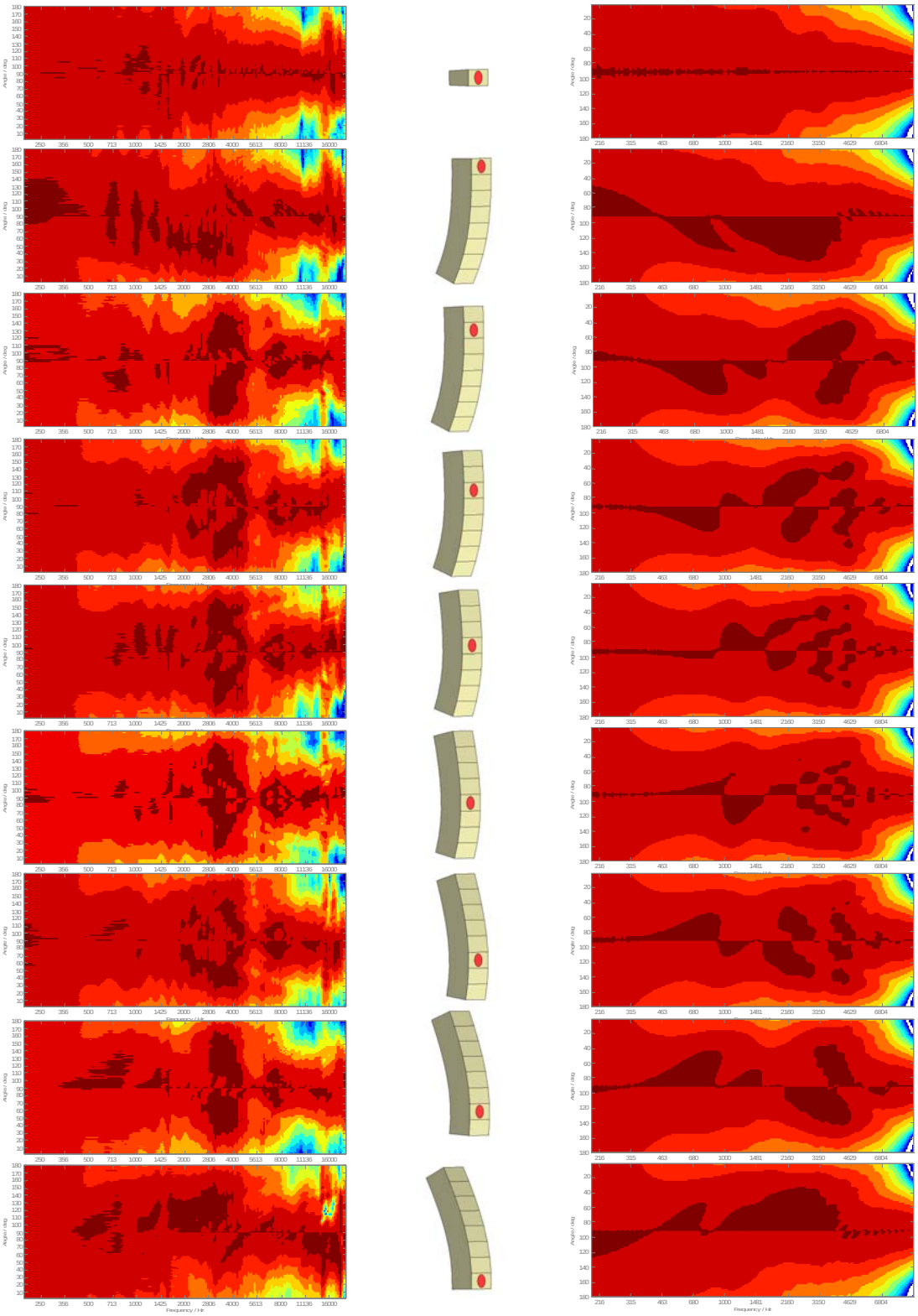

Figure 3

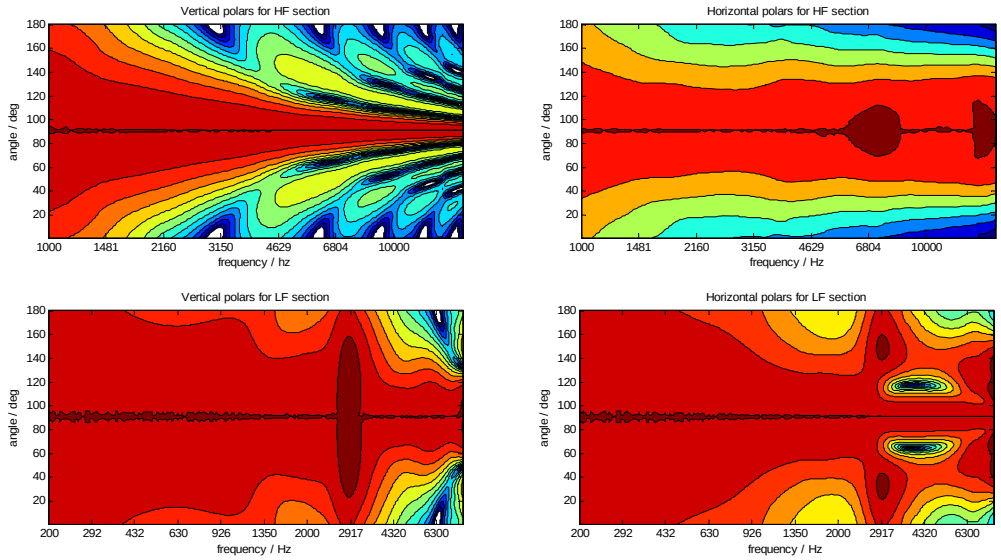

Figure 4 Signal processing applied each element

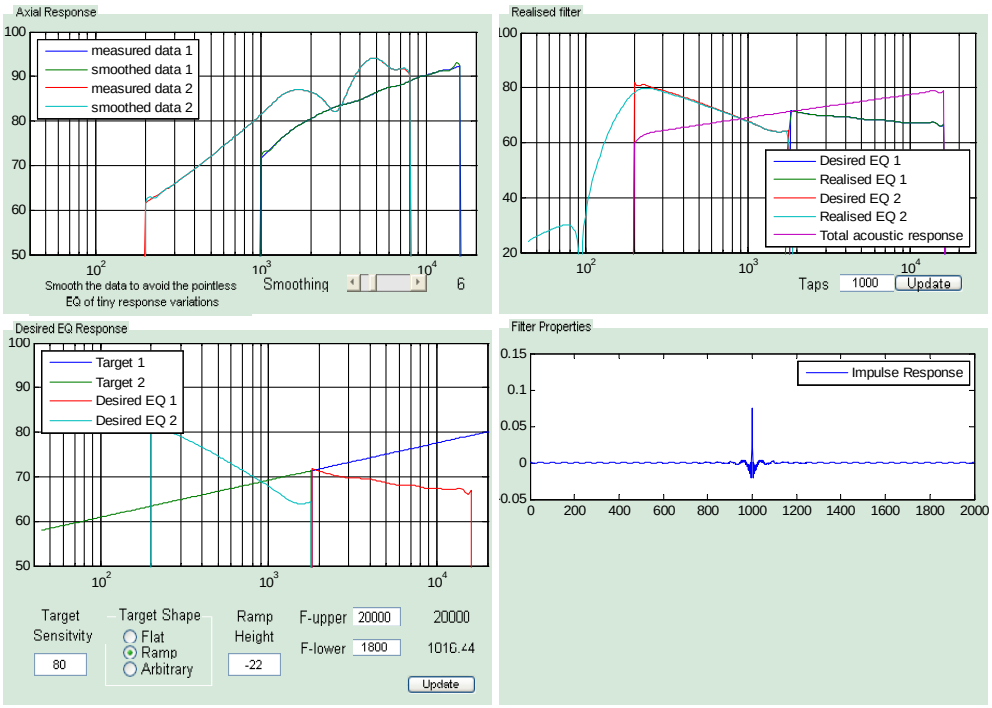

Figure 5

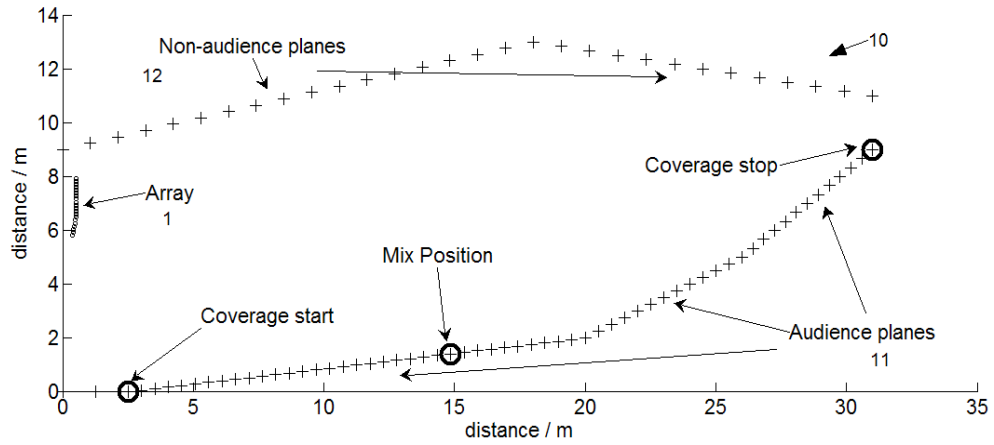

Figure 1

Table 1

Element	Manual array	Improved array with convex constraint (only C1>0)	Convex array with leakage and target (C3>C1)	Convex array with leakage and target (C3>>C1)	Convex array with leakage and target (C3>>>C1)	Direct splay angle manipulation (only C1>0)	Direct splay angle manipulation (C1>0 , C2>0)
1	8	8	8	8	8	8	8
2	0	0	0	1	1	0	1
3	1	2	1	1	1	2	2.5
4	1	2	1	1	1	2	2
5	2	2	2	1	1	2	1
6	2	2	2	1	1	2	1.5
7	2	2	2	1	1	2	2
8	3	2	2	1	1	2	2
9	3	2	2	2	1	1.5	2.5
10	3	2	2	2	1	2	2
11	4	2	2	2	2	2	2
12	4	3	2	2	2	3	3
13	4	3	2	2	2	2	3
14	5	4	3	3	2	3.5	4.5
15	5	4	3	3	3	3.5	4
16	5	5	4	4	3	4.5	4
17	6	5	5	5	4	6	5.5
18	6	6	5	5	5	6	5.5
19	6	6	6	6	5	6	5.5
20	6	6	6	6	5	5.5	6

Figure 6

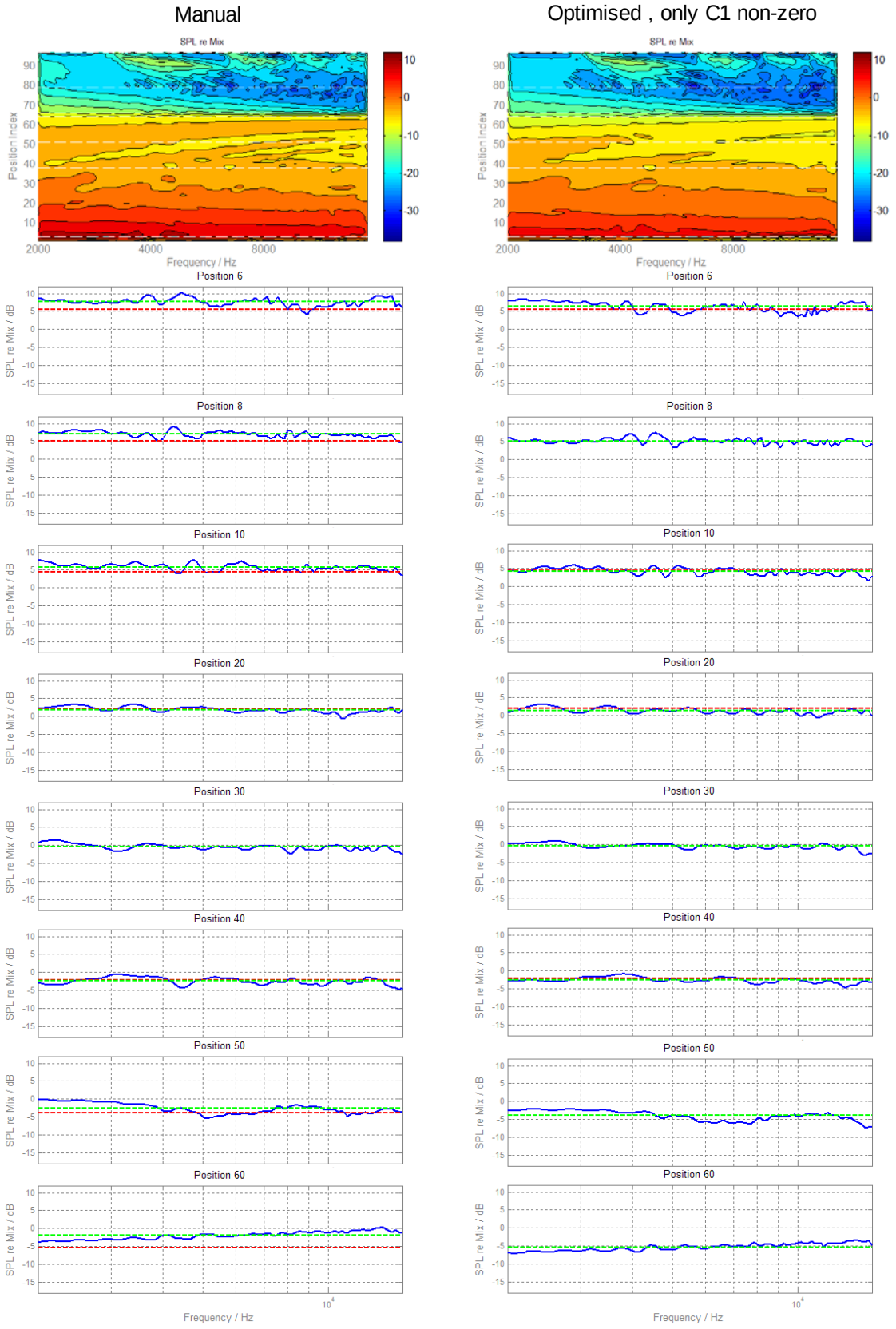
Manual
Optimised , only C1 non-zero
SPL re Mix
Position Index
Frequency / Hz
Position 6
Position 8
Position 10
Position 20
Position 30
Position 40
Position 50
Position 60
SPL re Mix / dB

Figure 7

C1 = 1 , C3 = 0

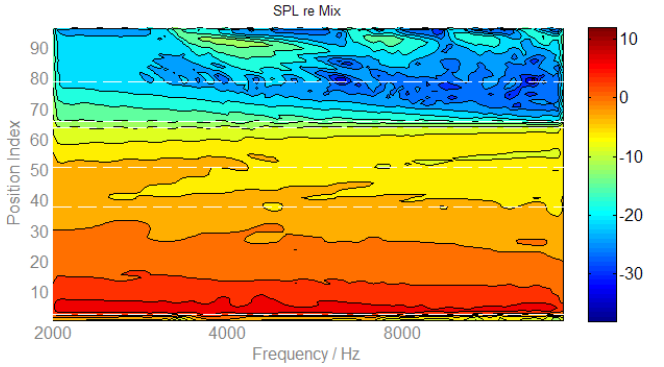

C1 = 1 , C3 > C1

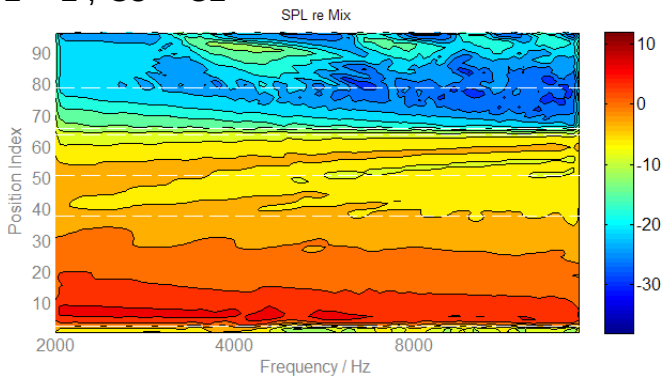

C1 = 1 , C3 >> C1

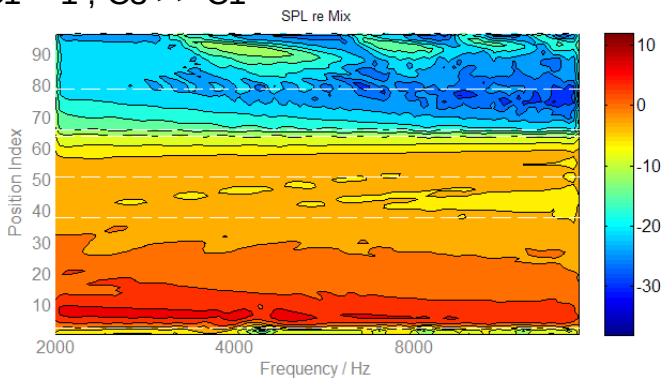

C1 = 1 , C3 >>> C1

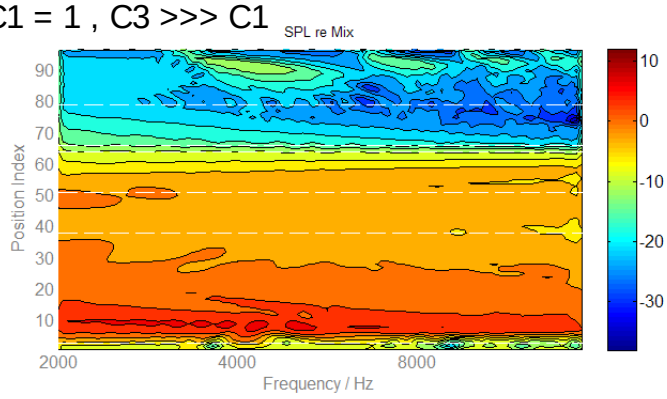

Figure 8

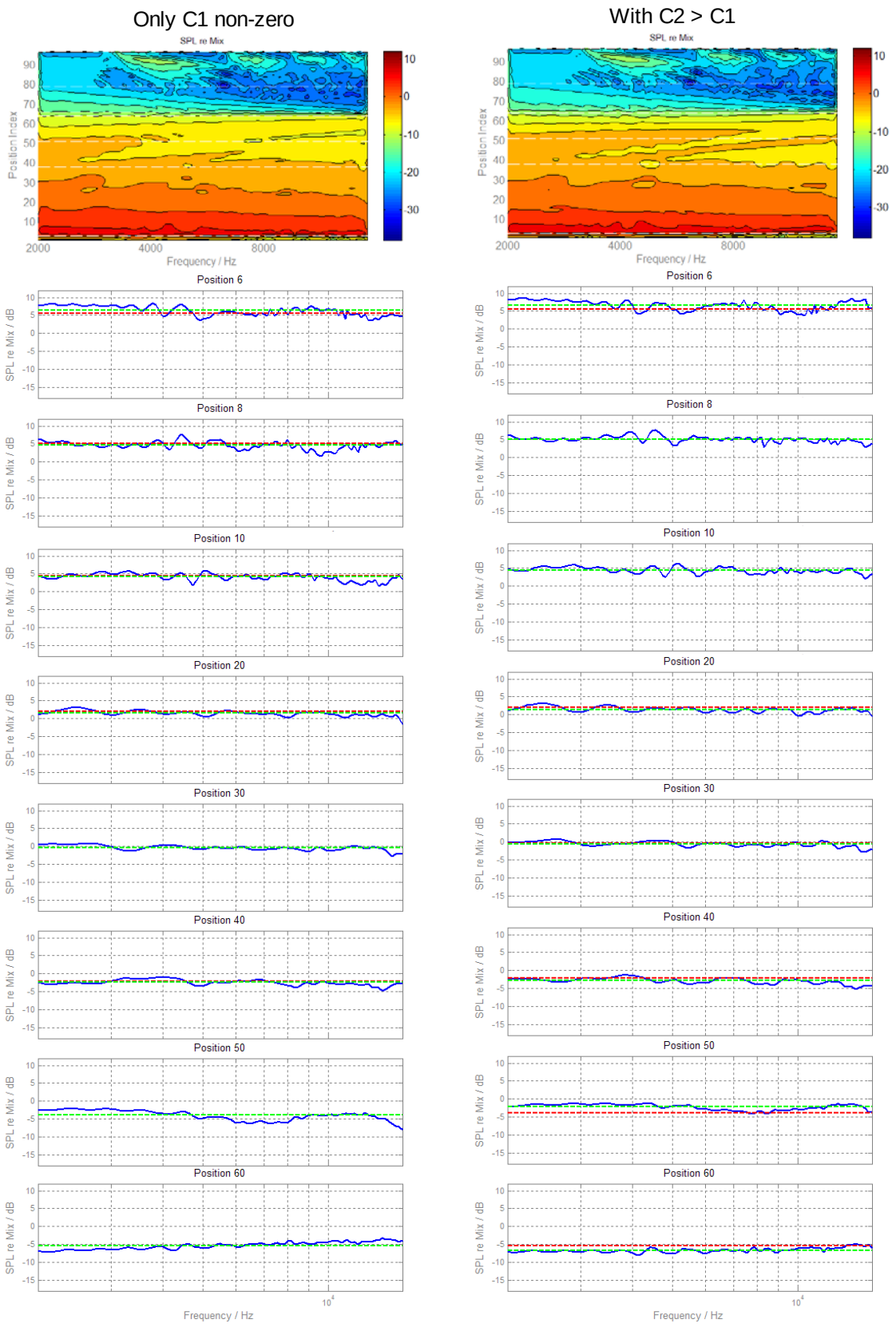
Only C1 non-zero
With C2 > C1
SPL re Mix
Position Index
Frequency / Hz
Position 6
Position 8
Position 10
Position 20
Position 30
Position 40
Position 50
Position 60
SPL re Mix / dB